

Carbon nanotube/metal interface studied by cross-sectional transmission electron microscopy

N. Y. Jin-Phillipp* and M. Rühle

Max-Planck-Institut für Metallforschung, Heisenbergstr. 3, D-70569 Stuttgart, Germany

(Received 17 August 2004; published 17 December 2004)

We present the first results on the interface between carbon nanotube (CNT) and metal by cross-sectional high-resolution transmission electron microscopy and spatially resolved electron energy loss spectroscopy on Fe-filled CNTs. The iron core is mainly single crystalline α -Fe. Under specific orientation relationships, a semicoherent CNT/Fe interface forms, where local lattice mismatch is accommodated by “interface dislocations.” A 0.2–0.4 eV energy shift of the π^* peak of the carbon K -edge towards higher values is found at the interface. The results prove experimentally an interfacial bonding between the CNT wall and Fe.

DOI: 10.1103/PhysRevB.70.245421

PACS number(s): 61.46.+w, 68.37.Lp, 73.20.-r, 81.07.De

I. INTRODUCTION

Since Iijima’s discovery of carbon nanotubes (CNTs)¹ by transmission electron microscopy (TEM), their structures have been extensively studied.² By combining various techniques available in TEM, e.g., high-resolution TEM (HRTEM) and analytical electron spectroscopy (AES), not only the structural but also the chemical and electronic information may be obtained. So far, most TEM investigations have been carried out on plan-view, i.e., the CNTs lie more or less in the image plane [Fig. 1(a)] with their axes perpendicular to the electron beam. Because of this limitation of imaging geometry a construction of a three-dimensional structure of a nanotube sometimes remains indefinite. Introducing other substances, such as metals,³ oxides,⁴ and even proteins,⁵ into the CNT system, or embedding the CNTs into a matrix⁶ offer possibility of developing new materials with specific properties and applications.⁷ It is expected that the atomic and electronic structures of interfaces between carbon nanotubes (CNTs) and other substances play important roles in the mechanical, chemical, and electronic properties of CNT composites. To study the structures of the interfaces between CNTs and other substances (filling or surrounding) is therefore of great interest and importance. For successful TEM in these cases, to investigate the CNTs and the interface edge-on by using cross-sectional specimens [Fig. 1(b)] is a necessity. In plan-view geometry [Fig. 1(a)] the weak interface signal would be smeared out by strong signals from the CNT wall and/or substances. Preparation of cross-sectional TEM specimens of CNTs is, however, a substantial challenge,⁸ especially for CNT composites owing to the marked differences in mechanical and chemical properties between CNT and other substances. In this paper we present the first results of HRTEM and spatially resolved electron energy-loss spectroscopy (EELS) studies on metal/CNT interfaces using cross-sectional specimens of Fe-filled multi-walled (MW) CNTs. Our results demonstrate experimentally the interfacial bonding between the filled Fe and the CNT wall.

II. EXPERIMENTS

The sample used for this study was grown by pyrolysis of organometallic precursors.⁹ Two methods were employed for

preparing the cross-sectional TEM specimens. Method one, the nanotubes were sandwiched between silicon wafers by using a small amount of epoxy. The sandwich was then sliced, mechanically ground and polished, and finally Ar⁺ ion milled with a final low-energy ion polishing. Method two, the CNTs were embedded in epoxy, and the mixture was then trimmed and finally thin sliced by an ultramicrotome. The latter method led sometimes to mechanical damage to the interface. Figure 1(c) shows a bright-field (BF) image of a cross-sectional TEM specimen prepared by ion thinning. CNTs showing circular shapes lie closely parallel to the electron beam, others are randomly aligned. For the present interface studies, the CNTs with circular cross sections were selected. A small tilt was often necessary in order to perfectly align the CNT axis parallel to the electron beam. HRTEM was performed on a JEOL 4000FX operated at 400 kV with point resolution of 0.2 nm and a JEOL 1250 atomic resolution microscope (ARM) operated at 1250 kV with a point resolution of 0.12 nm. During setting up optimal image conditions, areas away from that of interest were employed in order to minimize the electron radiation damage. Spatially resolved electron energy loss spectroscopy (EELS) was performed on a dedicated scanning transmission electron microscope VG HB501 operated at 100 kV. The probe diameter

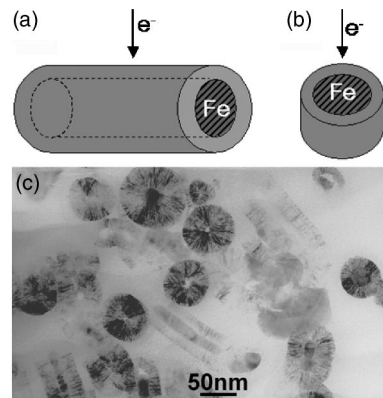


FIG. 1. Schematic of the geometry of (a) conventional plan-view TEM and (b) cross-sectional TEM. (c) BF image of a cross-sectional specimen.

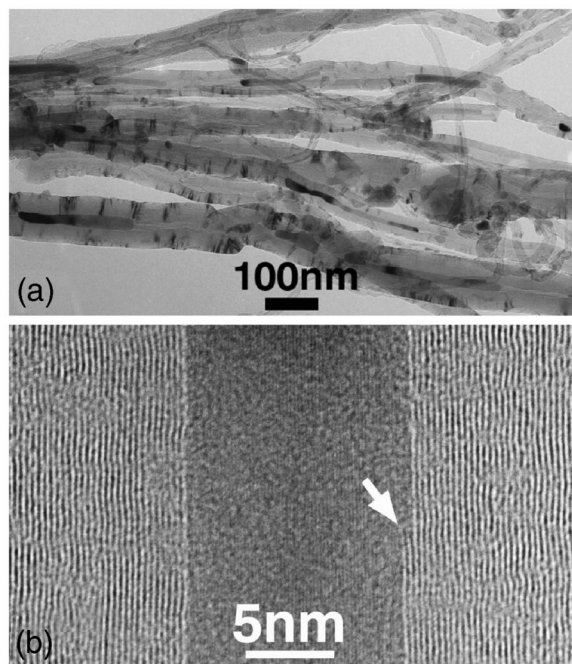


FIG. 2. (a) A bundle of Fe-filled MWCNTs, (b) HRTEM image of part of a CNT. The arrow indicates the ends of the innermost graphene layers.

was ~ 0.7 nm, and an energy dispersion of 0.2 eV/channel was chosen.

III. RESULTS AND DISCUSSION

Figure 2(a) shows a plan-view TEM image of a bundle of MWCNTs. The MWCNTs possess various diameters and are partly filled. HRTEM image of a small section of a CNT [Fig. 2(b)], where individual graphene sheets appear as dark fringes, reveals that the CNT wall is imperfect. Some graphene layers terminate in the middle of the wall as well as in the innermost of the wall, where the inner diameter of the MWCNT changes, as pointed out by an arrow. Figure 3(a) shows a cross section of a MWCNT with an empty core. The tube wall is quasicircular in cross section. However, it is difficult to find a complete circle of an individual graphene tube. Same as observed in the plan-view specimen (Fig. 2), the CNT walls are highly defective. This low crystallinity of the MWCNT walls is not due to electron radiation damage,¹⁰ since defects appear in the dispersed plan-view specimens at the very beginning of observation with 200 kV electrons. In some regions of the tube wall the defects arrange along radius, as indicated with arrowheads in Fig. 3(a). This arrangement of the defects, also clearly seen as radial dark lines in the BF image of Fig. 1(c), is very similar to the interlayer dislocation model suggested by Feng *et al.*¹¹ Figure 3(b) shows a HRTEM image of a cross section of a CNT filled with Fe. The characteristics of the CNT wall are very similar as that shown in Fig. 3(a). A lattice of single crystal is observed in the core of the nanotube, which consists of two sets of lattice fringes perpendicular to each other with a spacing of 0.19 nm and 0.20 ± 0.01 nm, respectively.

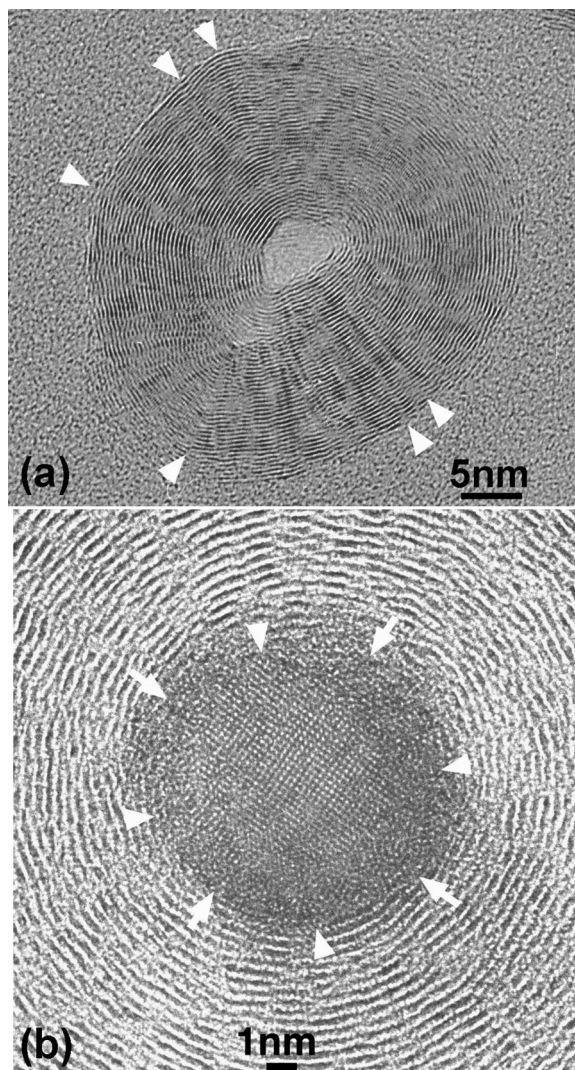


FIG. 3. (a) HRTEM of a cross section of a MWCNT with an empty core, showing defects in the walls arranged along the radius. (b) HRTEM of the central part of a cross section of a MWCNT filled with Fe.

This is consistent with the crystal structure of α -Fe close to a $\{100\}$ -pole axis, being tetragonally distorted owing to the C solution (martensite). In some CNTs other structures of the filling have been found, namely γ -Fe and FeC_x . Figure 4(a) shows a cross-sectional HRTEM image of another Fe-filled CNT. As in Fig. 3(b), the metal filling possesses a single crystalline structure. The central region of its core and two regions including the metal/CNT interface (marked with frames) are enlarged in Figs. 4(b), 4(c), and 4(d), respectively. In Fig. 4(b) three sets of the lattice planes are clearly seen with a spacing of 0.20 ± 0.01 nm, which make an angle of 60° with each other. This agrees with the α -Fe crystal structure along a $\langle 111 \rangle$ -zone axis. Note that the crystal structure extends up to the innermost graphene layer of the C wall. In Fig. 4(c), two controlling lines are drawn parallel to one set of $\{110\}$ planes of the Fe lattice in the center of the filling. Close to the interface the $\{110\}$ atomic planes are bent by an angle of $\sim 1^\circ$, indicating an elastic relaxation of the Fe lattice, which may be caused by its bonding with the

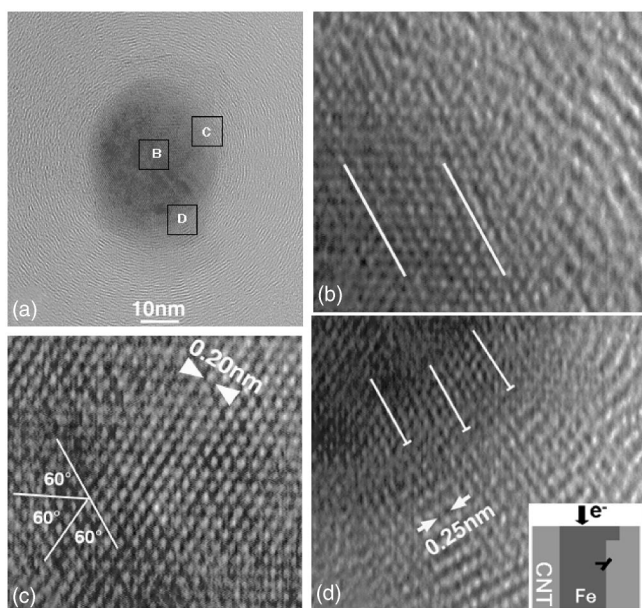


FIG. 4. (a) HRTEM of a cross section of a Fe filled CNT. (b) Lattice image of the central part of the Fe filling. (c) and (d) Interface region C and D marked in (a), respectively. The extra one half of the atomic planes of Fe, analogue to “interface dislocations,” are marked with \perp .

curved graphene sheet. In Fig. 4(d), in the C wall region fringes perpendicular to the graphene sheets of the CNT with a spacing of 0.25 nm are observed, which is twice the spacing of $\{110\}$ planes of graphite. It is interesting to note that in this region one set of Fe $\{110\}$ lattice planes is parallel to these fringes in the CNT wall region. This may be interpreted as the following: Part of the Fe core in this cross section has a different diameter, as schematically drawn in the inset of Fig. 4(d). Similar to the case of heterolayers, the Fe lattice in this extruded region elongate elastically in order to fit the graphite lattice beneath it. Because Fe has a higher atomic scattering factor than C, the contrast of these fringes in the C wall region is contributed mainly by the elongated Fe lattice. Extra atomic half-planes in the Fe core are observed with a spacing of six atomic planes. Such an atomic arrangement at Fe/CNT interface is analogous to “interface dislocations” in other heterostructures (e.g., Ref. 12). The $\{110\}$ spacing of α -Fe is 0.21 nm, smaller than the double $\{110\}$ spacing of graphite ($0.123 \text{ nm} \times 2 = 0.246 \text{ nm}$). In order to accommodate the lattice mismatch between graphite and Fe under this particular orientation relationship, these “interface dislocations” are expected to have a spacing of six atomic planes, which agrees with our experimental observation. Such type of semicoherent interface implies a chemical bonding between Fe and the CNT wall.

In order to study the electronic structure of the CNT/Fe interface, spatially resolved EELS was performed. Figure 5(a) shows BF and high-angle annular dark-field (HAADF) images of one cross section of a CNT. The contrast of the HAADF image, known as Z-contrast,¹³ arises mainly from different atomic scattering factors. Therefore, the HAADF image shows a strong bright contrast of the Fe core and a weak contrast of the C wall. The EELS line-scan is perpen-

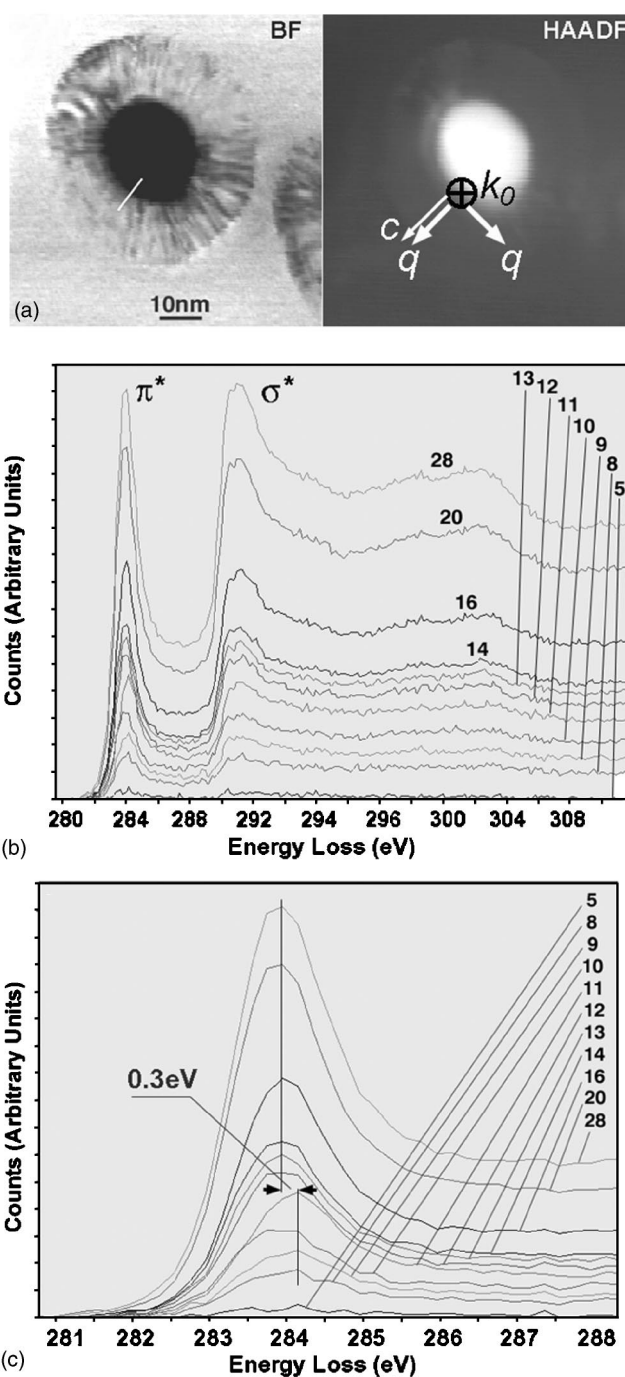


FIG. 5. Line-scan EELS spectroscopy on a cross section of a Fe-filled CNT. (a) BF and HAADF images. The position of the line-scan is shown in the BF image as a white line, and the scattering geometry is sketched in the HAADF image. (b) ELNES of carbon K -edge. The sequential numbers of the spectra are indicated. (c) A close look of the carbon π^* peaks. Note that the peak position of the π^* peak obtained from the interface region shows a shift of 0.3 eV towards higher energy in comparison with the spectra obtained from the C-wall region.

dicular to the interface, starting in the Fe region and extending symmetrically into both the Fe and C wall. The position of the scan is indicated with a white line in the BF image. Along the 10 nm long line 30 EELS spectra were recorded,

i.e., the spacing between sequential spectra is ~ 0.3 nm. It should be noted that, with this cross-sectional geometry the electron beam is parallel to the graphene layers along the CNT (\mathbf{k}_0), which gives rise to inelastic scattering events incorporating momentum transfers (\mathbf{q}) parallel as well as perpendicular to the local c axis of the layers, as sketched in Fig. 5(a). Figure 5(b) shows the background subtracted energy loss near-edge structure (ELNES) of the C K -edge of the selected spectra. No C signal was detected in spectra 1–4 taken in the Fe region (not shown here). In the spectra taken from the CNT wall region, the ELNES resembles closely that of graphite: a π^* peak close to 284 eV, corresponding to the $1s$ - π^* transition, and a main peak setting on at ~ 290 eV, corresponding to $1s$ - σ^* transition. The relative σ^* peak intensity is markedly lower than in graphite. This agrees with the observation of Stéphan *et al.*,¹⁴ that in plan-view geometry the intensity ratio π^*/σ^* is higher near the edge position than for the central positions. In both our cross section and their plan-view edge position geometries scattering events incorporate momentum transfers parallel to the local c axis of the graphene layer, in contrast with their plan-view central position, where the momentum transfer is perpendicular to the local c axis. The less detailed σ^* peak may be attributed to the highly defective nature of the C wall (Fig. 3), and the end-on geometry of the graphene sheets may have a similar effect.¹⁴

It is particularly interesting to note in Fig. 5(c) that the π^* peak position of the spectra taken in the Fe/CNT interface region (spectra 8–11) is at higher energy than in spectra taken from the C wall region (spectra 13–30). Measurements from several CNTs show that the energy shift of the π^* peak ranges from 0.2 to 0.4 eV. A close look at the on-set of the σ^* peak has shown a similar shift towards higher energies in spectra taken close to the interface. Considering the diameter of the electron beam (≤ 1 nm), together with beam broadening during the penetration through the specimen, and the spacing of 0.3 nm between sequential EELS spectra, we estimate that five to six spectra contain CNT/Fe interface specific signal in one EELS line scan. However, due to the strong C signal from the C-wall, the weak interfacial signal is expected to be recognizable only in a few spectra, which are taken at the interface region on the Fe side. This agrees with our experimental observations. We believe, therefore, that this shift of the π^* peak towards higher energy arises due to the Fe/CNT interface.

When the metallic Fe crystal filled in the core of a MWCNT and the C inner graphene layer of the MWCNT form an interface, the dominant interaction is expected for that of the Fe $3d$ orbital with the local carbon π orbital. Electron states of Fe may populate the energy gap between π and π^* of the CNT. Charge transfer and the induced interfacial field determine position of the band structure of the CNT relative to the metal Fermi level. A detailed *ab initio* calculation is needed to clarify quantitatively how the overlap and hybridization of the electronic states of Fe electron states with C states affect the C band structure at the interface. For single-wall (SW) CNT supported on a gold substrate, calculation of Xue and Datta¹⁵ has shown that the electron charge transfer from SWCNT to the gold substrate induces a local electronic potential perturbation which gives rise to a Fermi

level shift of ~ 0.2 eV towards the valence band, which explains the Fermi level shift in scanning tunneling spectroscopy measurements using a scanning tunneling microscope.¹⁶ For the system of a $3d$ transition-metal deposited on the graphite substrate, on the other hand, theoretical calculations¹⁷ have predicted that a strong hybridization of Fe $3d$ orbital with C π orbital results in a small electron charge transfer from Fe adatoms (and dimers) to the graphite substrate. Assuming that the same type of charge transfer occurs in the case of the Fe crystal filled in CNT, one would expect, in comparison with the case of SWCNT on gold, a Fermi level shift to the opposite direction, i.e., towards the conduction band of the CNT. The excitation of a C $1s$ electron at the interface to the empty π^* would require, therefore, higher energy. Our observation of a shift of π^* peak position towards higher energies proves, therefore, the interfacial bonding between the Fe filling and CNT wall. We have also noted, however, that some EELS line scans do not exhibit any significant change of the π^* peak position when the electron beam crosses the interface. According to our HR-TEM observation, the orientation relationship between the inner graphene layer of a CNT wall and the Fe crystal may vary from one CNT to the other [e.g., compare Fig. 3(b) with Fig. 4(a)], as well as at various positions along the circular interface of the same CNT. For example, local c axis of graphene layers of the MWCNT in Fig. 3(b) can be parallel to $\langle 011 \rangle$ (arrows) and $\langle 010 \rangle$ (arrowheads). Differences in the bonding between Fe and CNT at various interface positions may, therefore, be expected. This is unlike the case of a CNT coated with a thin layer of SiO_x ,¹⁸ where the bonding does not change along the circular interface. Besides, FeC_x filling, also observed in our sample, may have a different interface with CNT.

Finally, we would like to mention that, since the CNTs used in our study are highly defected, whether the formation of the interfacial bonding is assisted by the defects present in the CNT walls needs further investigations. To fabricate perfect CNTs filled with metal for the future study is essential. We have also found trace of O at the interface and Fe filling, especially when we perform a second time EELS line scan on the same CNT cross section (crossing another part of the circular interface).

IV. CONCLUSION

Our results constitute, to the best of our knowledge, the first cross-sectional HRTEM and high-spatially resolved EELS study of an interface in a CNT composite. Elastic relaxation of the Fe crystal takes place close to the CNT/Fe interface. Under a particular orientation relationship, a semi-coherent interface forms, and “interface dislocations” accommodate the lattice mismatch between Fe and graphite. The π^* peak of the carbon K -edge of EELS shifts 0.2–0.4 eV towards higher values. These results demonstrate experimentally the interfacial bonding between filled Fe and CNT wall. We believe that cross-sectional HRTEM and EELS, together with structural modeling and image simulation, will play an important role in future studies on atomic and electronic structures of the interfaces in various CNT composite systems.

ACKNOWLEDGMENTS

One of the authors (N.Y.J.) acknowledges stimulating discussions with Dr. W. Sigle and Professor F. Banhart, Johannes Gutenberg-Universität Mainz. The authors are

grateful to Dr. Grobert, University of Oxford, for providing the sample, to M. Kelsch and M. Sycha for TEM specimen preparations, and to J. Thomas and R. Höschel for their assistance in TEM experiments.

*Author to whom correspondence should be addressed. Electronic address: nyjin@mf.mpg.de

¹S. Iijima, *Nature (London)* **345**, 56 (1991).

²*Electron Microscopy of Nanotubes*, edited by Z. L. Wang and C. Hui (Kluwer Academic, Berlin, 2003).

³M. Ajayan and S. Iijima, *Nature (London)* **361**, 333 (1993).

⁴S. C. Tsang, Y. K. Chen, P. J. F. Harris, and M. L. H. Green, *Nature (London)* **372**, 159 (1994).

⁵S. C. Tsang, J. J. Davis, M. L. H. Green, H. Allen, A. O. Hill, Y. C. Leung, and P. J. Sadler, *J. Chem. Soc., Chem. Commun.* **17**, 1803 (1995).

⁶R. Z. Ma, J. Wu, B. Q. Wei, J. Liang, and D. H. Wu, *J. Mater. Sci.* **33**, 5243 (1998).

⁷M. Terrones, *Annu. Rev. Mater. Res.* **33**, 419 (2003).

⁸P. M. Ajayan, O. Stephan, C. Colliex, and D. Truth, *Science* **265**, 1212 (1994).

⁹M. Mayne, N. Grobert, M. Terrones, R. Kamalakaran, M. Rühle,

H. W. Kroto, and D. R. M. Walton, *Chem. Phys. Lett.* **338**, 101 (2001).

¹⁰F. Banhart, *Chem. Phys. Lett.* **269**, 349 (1997).

¹¹S. Q. Feng, D. P. Yu, G. Hu, X. F. Zhang, and Z. Zhang, *J. Phys. Chem. Solids* **58**, 1887 (1997).

¹²N. Y. Jin-Phillipp, W. Sigle, A. Black, D. Babic, E. Hu, and M. Rühle, *J. Appl. Phys.* **89**, 1017 (2001).

¹³S. J. Pennycook and D. E. Jesson, *Phys. Rev. Lett.* **64**, 938 (1990).

¹⁴O. Stephan, P. M. Ajayan, C. Colliex, F. Cyrot-Lackmann, and E. Sandre, *Phys. Rev. B* **53**, 13824 (1996).

¹⁵Y. Xue and S. Datta, *Phys. Rev. Lett.* **83**, 4844 (1999).

¹⁶J. W. G. Wildöer, L. C. Venema, A. G. Rinzler, R. E. Smalley, and C. Dekker, *Nature (London)* **391**, 59 (1998).

¹⁷D. M. Duffy and J. A. Blackman, *Phys. Rev. B* **58**, 7443 (1998).

¹⁸N. Grobert, T. Seeger, G. Seifert, and M. Rühle, *J. Ceram. Proc. Res.* **4**, 1 (2003).